Supporting Information for

Original article

Non-canonical STING–PERK pathway dependent epigenetic regulation of vascular endothelial dysfunction *via* integrating IRF3 and NF-*κ*B in inflammatory response

Xuesong Li[a,†], Xiang Chen[a,†], Longbin Zheng[a,b,†], Minghong Chen[a], Yunjia Zhang[a], Ruigong Zhu[a], Jiajing Chen[c], Jiaming Gu[a], Quanwen Yin[a], Hong Jiang[a], Xuan Wu[a], Xian Ji[a], Xin Tang[a], Mengdie Dong[a], Qingguo Li[d,*], Yuanqing Gao[a,*], Hongshan Chen[a,d,e,f,*]

[a]*Key Laboratory of Cardiovascular and Cerebrovascular Medicine, School of Pharmacy, Nanjing Medical University, Nanjing 211166, China*

[b]*Department of Anesthesiology, Sir Run Run Hospital, Nanjing Medical University, Nanjing 211166, China*

[c]*Department of Pharmacy, Huashan Hospital, Fudan University, Shanghai 200040, China*

[d]*Department of Cardiothoracic Surgery, The Second Affiliated Hospital of Nanjing Medical University, Nanjing 211166, China*

[e]*Key Laboratory of Targeted Intervention of Cardiovascular Disease, Collaborative Innovation Center for Cardiovascular Disease Translational Medicine, Nanjing Medical University, Nanjing 211166, China*

[f]*Department of Cardiology, Huai'an First People's Hospital affiliated with Nanjing Medical University, Huai'an 223399, China*

Received 10 May 2023; received in revised form 6 July 2023; accepted 2 August 2023

*Corresponding authors. Tel.: +86 25 86868467.

E-mail addresses: hongshanchen@njmu.edu.cn (Hongshan Chen), yuanqinggao@njmu.edu.cn (Yuanqing Gao), lqg0235062@163.com (Qingguo Li).

†These authors made equal contributions to this work.

1. Supporting tables

Table S1 PCR primers used in this study.

Factor or PTM	Forward	Reverse
	Human	
ISG15	CACCTGAAGCAGCAAGTGAG	ATTTCCGGCCCTTGATCCTG
ISG20	CTCTACGCCATCACTGGGTC	CTCTTCGTCTGATCCGTCCT
MX2	TCTGGGGAAAGCTAGGGGAA	TCTGGGGAAAGCTAGGGGAA
IL-6	CCTCCAGAACAGATTTGAGAGTAGT	GGGTCAGGGGTGGTTATTGC
IL-1β	TTGCCAGCCAGTGACACAAT	GAGAAGGTGGTTGTCTGGGAAT
CCL2	GATCTCAGTGCAGAGGCTCG	TCTGGGGAAAGCTAGGGGAA
ICAM-1	AGGTTGAACCCCACAGTCAC	TCTGAGACCTCTGGCTTCGT
VCAM-1	CACTGAATGGGAAGGTGACG	ACACTTGACTGTGATCGGCTT
SELE	AAGCTGTGAGATGCGATGCT	GATCTTTCCCGGAACTGCCA
MT-ND1	CTCTTCGTCTGATCCGTCCT	TGAGGTTGCGGTCTGTTAGT
MT-ND2	GTAGACAGTCCCACCCTCAC	TTGATCCCGTTTCGTGCAAG
L1ORF1	AGAACGCCACAAAGATACTCCTCG	CTCTCTTCTGGCTTGTAGGGTTTCTG
L1ORF2	AAACTGAACAACCTGCTCCTGAATG	CTACACACTGCTTTGAATGCGTCC
RNA18S	GTAACCCGTTGAACCCCATT	CCATCCAATCGGTAGTAGCG
	Mice	
Il-6	TGATGGATGCTACCAAACTGGA	GGAGAGCATTGGAAATTGGGG
Il-1β	TAATGCTTGAGCCCACCCTG	GGGGGAGGCTTCTCTACTGA
Ccl2	GGCTCAGCCAGATGCAGTTA	TCATTTGGTTCCGATCCAGGTT
Icam-1	AAACCAGACCCTGGAACTGC	CCCATGGGAGCTAAAGGCAT
Vcam-1	TATGTCAACGTTGCCCCCAA	AAATGCCGGAATCGTCCCTT
Sele	ATGGAAGCCTGAACTGCTCC	TGTCGTGTTCCATGGGTAGC
mt-Nd1	CAAACACTTATTACAACCCAAGAACA	TCATATTATGGCTATGGGTCAGG
mt-Nd2	CCATCAACTCAATCTCACTTCTATG	GAATCCTGTTAGTGGTGGAAGG
L1 gDNA	TAGGAAATTAGTTT GAATAGGTGAGAGGGT	TCCAGAAGCTGTCAGGTTCTCTGGC
Sting	TCGCACGAACTTGGACTACTG	CCAACTGAGGTATATGTCAGCAG

Table S2 Clinical characteristics of the patients recruited are shown.

Type	Patient	Sex	Age	Approach	Size (mm)	Location	Calcification
Atherosclerotic aortic specimens	1	Female	65	Endarterectomy specimens	6 × 10	Carotid intima	No
	2	Male	57	Endarterectomy specimens	8 × 20	Carotid intima	No
	3	Male	60	Endarterectomy specimens	5 × 14	Carotid intima	No
Non-atherosclerotic aortic specimens	1	Male	53	Coronary artery bypass surgery	20 × 10	Left internal thoracic artery	No
	2	Female	48	Heart transplantation	45 × 10	Aortic arch	No
	3	Male	64	Coronary artery bypass surgery	5 × 10	Left internal thoracic artery	No

Table S3 Antibodies used in this study.

Factor or PTM	Vendor	Cat Number
p-STING	Cell Signaling Technology	50907S
p-STING	Cell Signaling Technology	72971
STING	Cell Signaling Technology	13647
STING	Invitrogen	PA5-20782
p-TBK1	Cell Signaling Technology	5483T
TBK1	Cell Signaling Technology	38066
p-IRF3	Cell Signaling Technology	29047
IRF3	Invitrogen	712217
IRF3	Proteintech	11312-1-AP
Actin	Bioworld	AP0060
IgG	Cell Signaling Technology	3900
cGAS	Santa	sc-515777
p-p65	Cell Signaling Technology	3033
p65	Cell Signaling Technology	8242
BRD2	Cell Signaling Technology	5848S
BRD3	Invitrogen	PA5-30263
BRD4	Abcam	ab243862
H3K27ac	Abcam	ab177178
H3K4me1	Abcam	ab176844
H3K27me3	Abcam	ab6002
H3	Abcam	ab1791
ICAM-1	Santa	sc-8439
VCAM-1	Abcam	ab134047
dsDNA	Abcam	ab27156
dsDNA	Abcam	ab273137
Tomm20	Abcam	ab-78547
Tomm20	Proteintech	11802-1-AP
VDAC1	Abcam	ab14734
CD31	Abcam	ab24590
HRP-conjugated goat anti-rabbit secondary antibody	Jackson Labs	111035003
HRP-conjugated goat anti-mouse secondary antibody	Jackson Labs	115036003

Table S4 ChIP primers used in this study.

Primer set name	Forward sequence	Reverse sequence
	Human	
ICAM-1 (-1 kb)	GTGGATGTCGAGTCTTGGGG	CAACTCGAACCCAGGCTCAT
ICAM-1 (p)	GGGGCTAGAGACAGCGATT	CTTGTTGGGTTGGCACAGAG
ICAM-1 (+1 kb)	CGTGTCCTGTGTGAGTGGG	TTTTCTGGCCACGTCCAGTT
VCAM-1 (-1 kb)	AACTTGGCTGGGTGTCTGTT	TCTTGTTGCAGAGGCGGAG
VCAM-1 (p)	GCTCAGATTGGTGACTCCGT	GCTCTCTCTCATGTTGGCCTT
VCAM-1 (+1 kb)	GGCGCCTATACCATCCGAAA	ACCACAGCTCCATTTTGCCA
IL-6 (-1 kb)	CCTTAGAGCCTGGTGTCTGC	TCTGGGGGTTGGAGATGGAT
IL-6 (p)	ATAGCCCAGAGCATCCCTCC	GCTACATTTGCCGAAGAGCC
IL-6 (+1 kb)	CTATCCGGCCCAAGCTTTCT	TGGCCCATTTGGGTTTCTCA
IL-1β (-1 kb)	GGCTAGGGTAACAGCACCTG	CTGGGGCAGAGAACATACGG
IL-1β (p)	CCAGCTCTCCTAGCCAATAC	TGAGTGACTTCCCCATGACG
IL-1β (+1 kb)	TGTACCTGTCCTGCGTGTTG	CCAGCTTTTCCTAGGGATGGG
CCL2 (-1 kb)	CCCGGGGTAACTGAGGATTC	TAGGCTCTGGCACAAACCTG
CCL2 (p)	AGCATGAAAGTCTCTGCCGC	GAGAAGAAGAGGGGGCCTTAC
CCL2 (+1 kb)	TGGGAAAACTGAGGCACCAAG	CCATTCTGCACCAAAGGGCT
SELE (-1 kb)	TGAACACAGAAAGACCAGTGCT	ACTGTCAGCAGACCTGAACG
SELE (p)	GGTAGCACCATCTCACGTCC	ATGACACCATCTGCACCAGG
SELE (+1 kb)	AGCCATGCTTGTGCTCTGAT	CCCTGCTCCCTCCCTAAGAT
	Mice	
Icam-1 (-1 kb)	CTAGTGCCAAGTGGGTGGAG	TTAACCCACCAGACATGCCC
Icam-1 (p)	TAACGGGAAGTGGGATTGGA	ACCCATGGAGTGATGCTACG
Icam-1 (+1 kb)	TCTGTCTCTACCACACAGACCA	CATCACGAGGCCCACAATGA

Table S5 siRNA sequences used in this study.

Factor or PTM	Forward sequence	Reverse sequence
STING-1	GCAGCUGGGACUGCUGUUAAA	UAACAGCAGUCCCAGCUGCAG
STING-2	GCAGAGCUAUUUCCUUCCACA	UGGAAGGAAAUAGCUCUGCUG
STING-3	GCAUUACAACAACCUGCUACG	UAGCAGGUUGUUGUAAUGCUG
IRF3-1	GGCUGGUGUCGCAGCUGGACC	UCCAGCUGCGACACCAGCCAG
IRF3-2	GGAGCAAGGACCCUCACGACC	UCGUGAGGGUCCUUGCUCCGG
IRF3-3	GCCUCGAGUUUGAGAGCUACC	UAGCUCUCAAACUCGAGGCUG
p65-1	AGCGCAUCCAGACCAACAACA	UUGUUGGUCUGGAUGCGCUGA
p65-2	UGGAUUCAUUACAGCUUAAUC	UUAAGCUGUAAUGAAUCCAUG
p65-3	GCUGCAGUUUGAUGAUGAAGA	UUCAUCAUCAAACUGCAGCUG
BRD4-1	AGCCCAAGAGGCAGACCAACC	UUGGUCUGCCUCUUGGGCUUG
BRD4-2	GAAGAAACCGAGAUCAUGAUA	UCAUGAUCUCGGUUUCUUCUG
BRD4-3	GAUGUAAGAUACAAGUAUAUA	UAUACUUGUAUCUUACAUCUU

2. Supporting figures

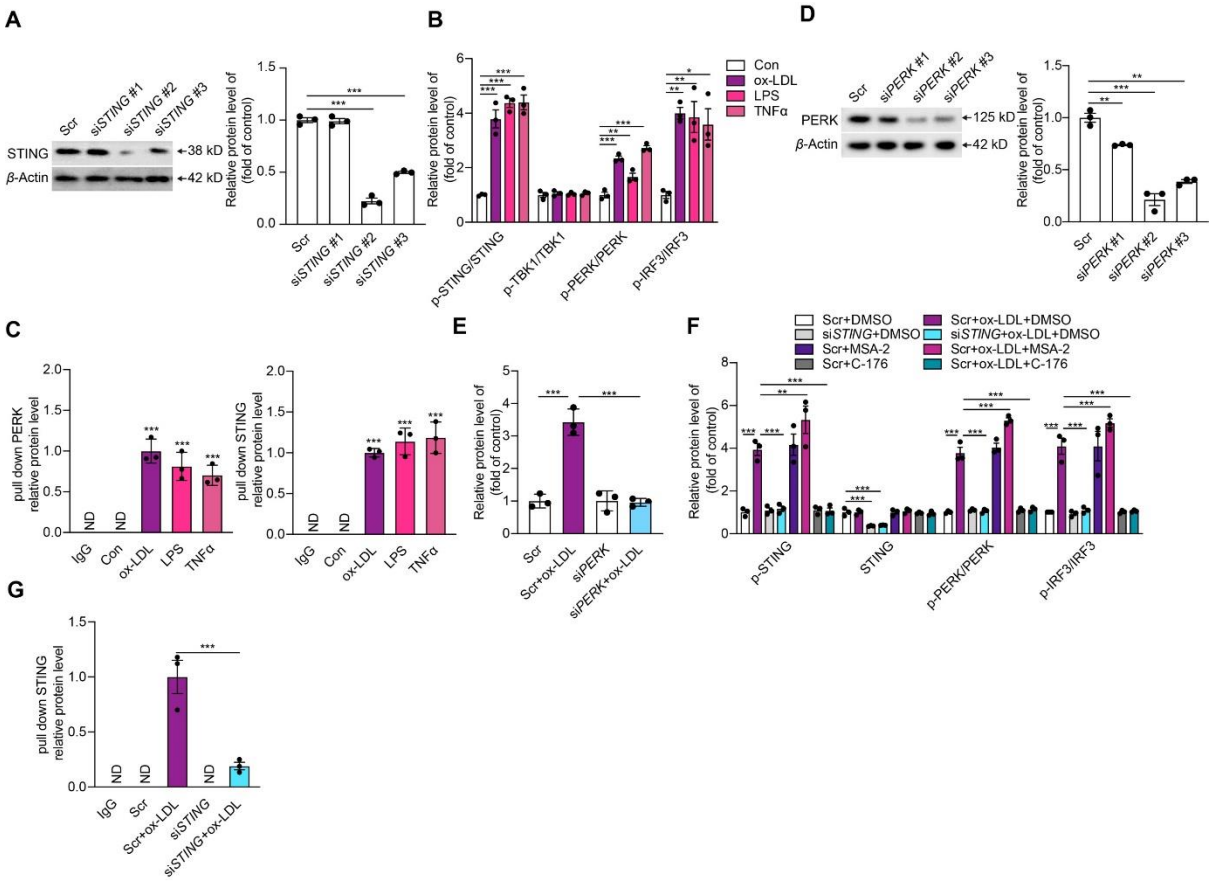

Figure S1 Activation of the non-canonical STING–PERK pathway in ox-LDL induced endothelial injury. (A) Western blot analysis of interference efficiency targeting STING in HCAECs. (B) Quantification of western blot data of Fig. 1F. (C) Quantification of western blot data from Fig. 1G. (D) Western blot analysis of interference efficiency targeting PERK in HCAECs. (E) Quantification of western blot data from Fig. 1H (p-IRF3/IRF3). (F) Quantification of western blot data from Fig. 1J. (G) Quantification of western blot data from Fig. 1K. Data are shown as mean ± SEM, $n = 3$; *$P < 0.05$, **$P < 0.01$, ***$P < 0.001$; ND, not detected.

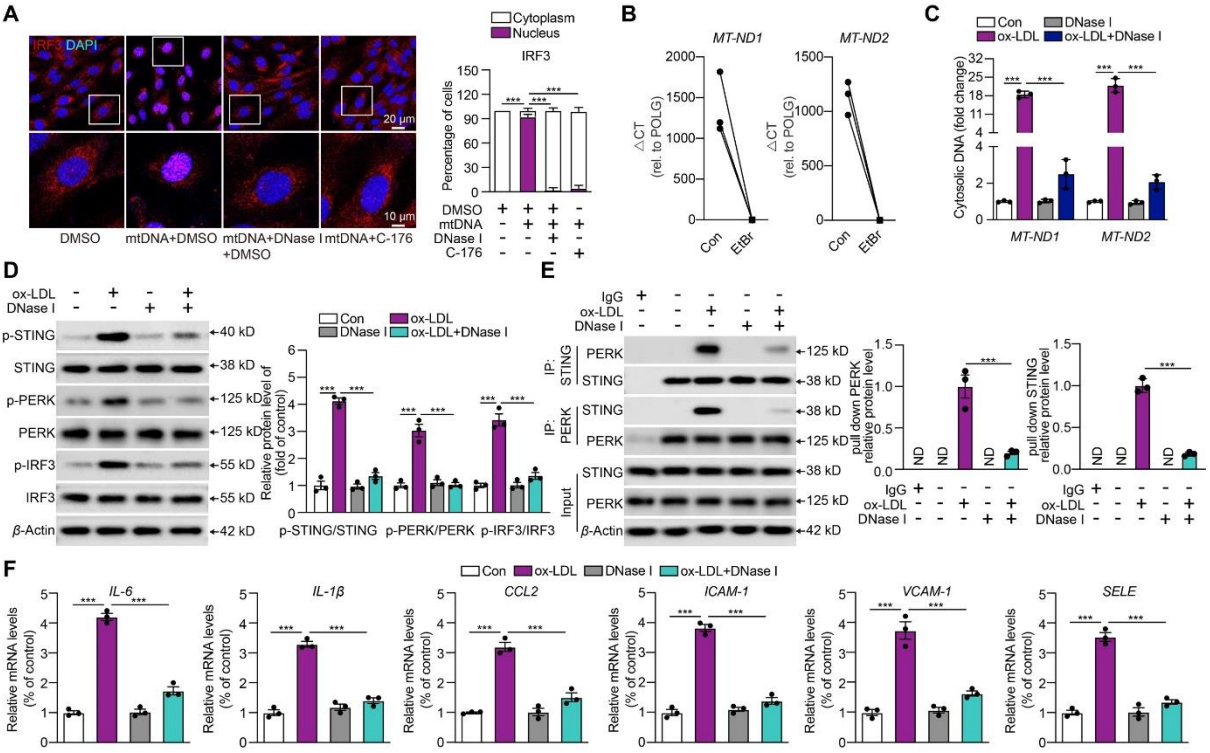

Figure S2 DNase I could effectively ameliorate the oxidized LDL-induced endothelial injury *via* inhibiting the non-canonical STING–PERK pathway activation. (A) Immunofluorescence staining of IRF3 (Scale bar = 20 μm). (B) qPCR analysis of mtDNA deletion efficiency by EtBr. (C) The qPCR analysis of the cytoplasmic mtDNA content of ox-LDL-treated HCAECs combined with DNase I (1 μg/mL). (D)–(F) Western blot analysis of the non-canonical STING–PERK pathway (D), co-immunoprecipitation analysis of STING-PERK binding (E), and adhesions molecules and chemokines mRNA expression (F) in ox-LDL-treated HCAECs combined with DNase I. Data are shown as mean ± SEM, $n = 3$; ***$P < 0.001$; ND, not detected.

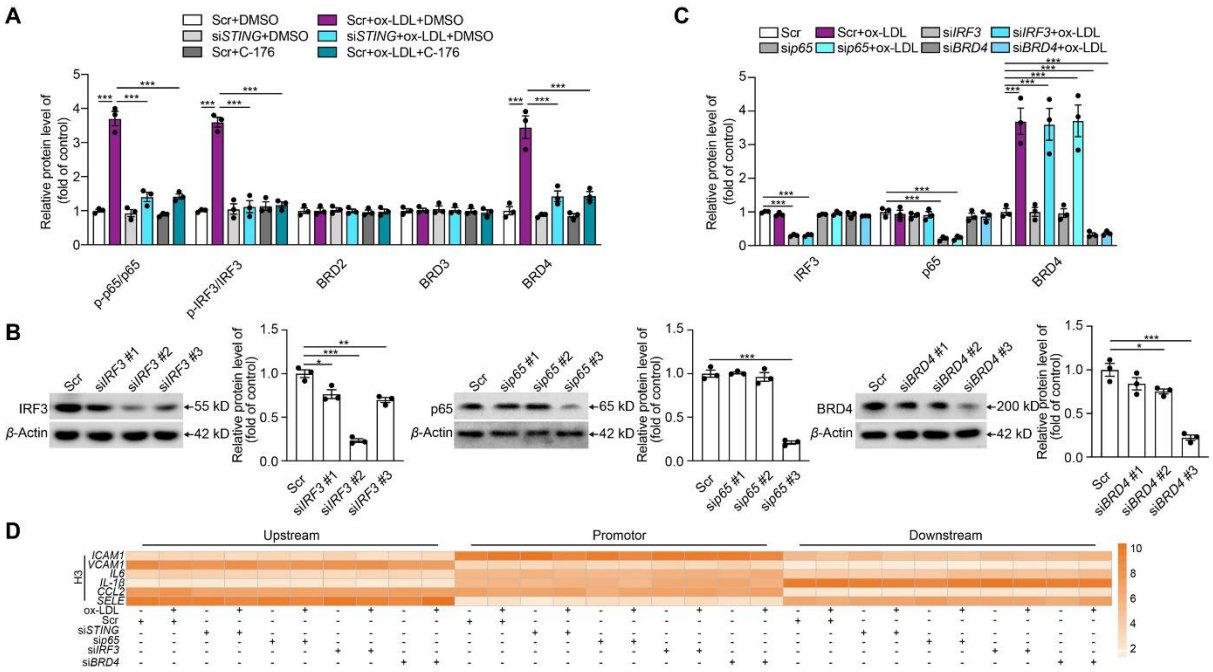

Figure S3 The interference efficiency of proteins. (A) Quantification of western blot data of Fig. 4B. (B) Western blot analysis of interference efficiency targeting IRF3, p65 and BRD4 in HCAECs. (C) Quantification of western blot data of Fig. 4C. (D) H3 was pulled down as the ChIP control for the tested proteins (Fig. 4D). Data are shown as mean ± SEM, $n = 3$; $^{*}P < 0.05$, $^{**}P < 0.01$, $^{***}P < 0.001$.

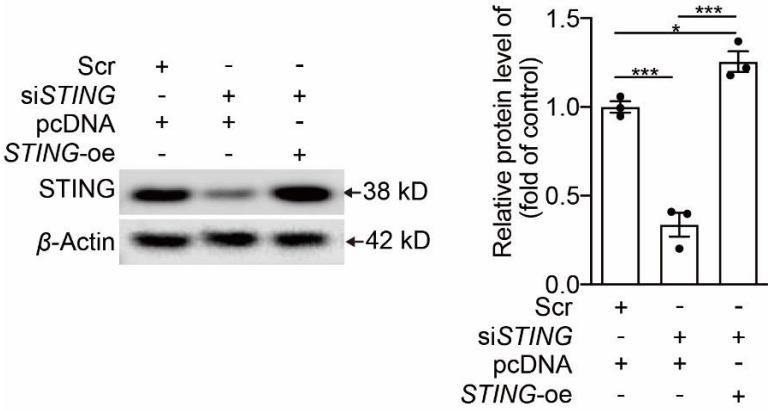

Figure S4 Western blot analysis of interference efficiency and overexpression efficiency targeting STING in HCAECs. Data are shown as mean ± SEM, $n = 3$; $^{*}P < 0.05$, $^{***}P < 0.001$.

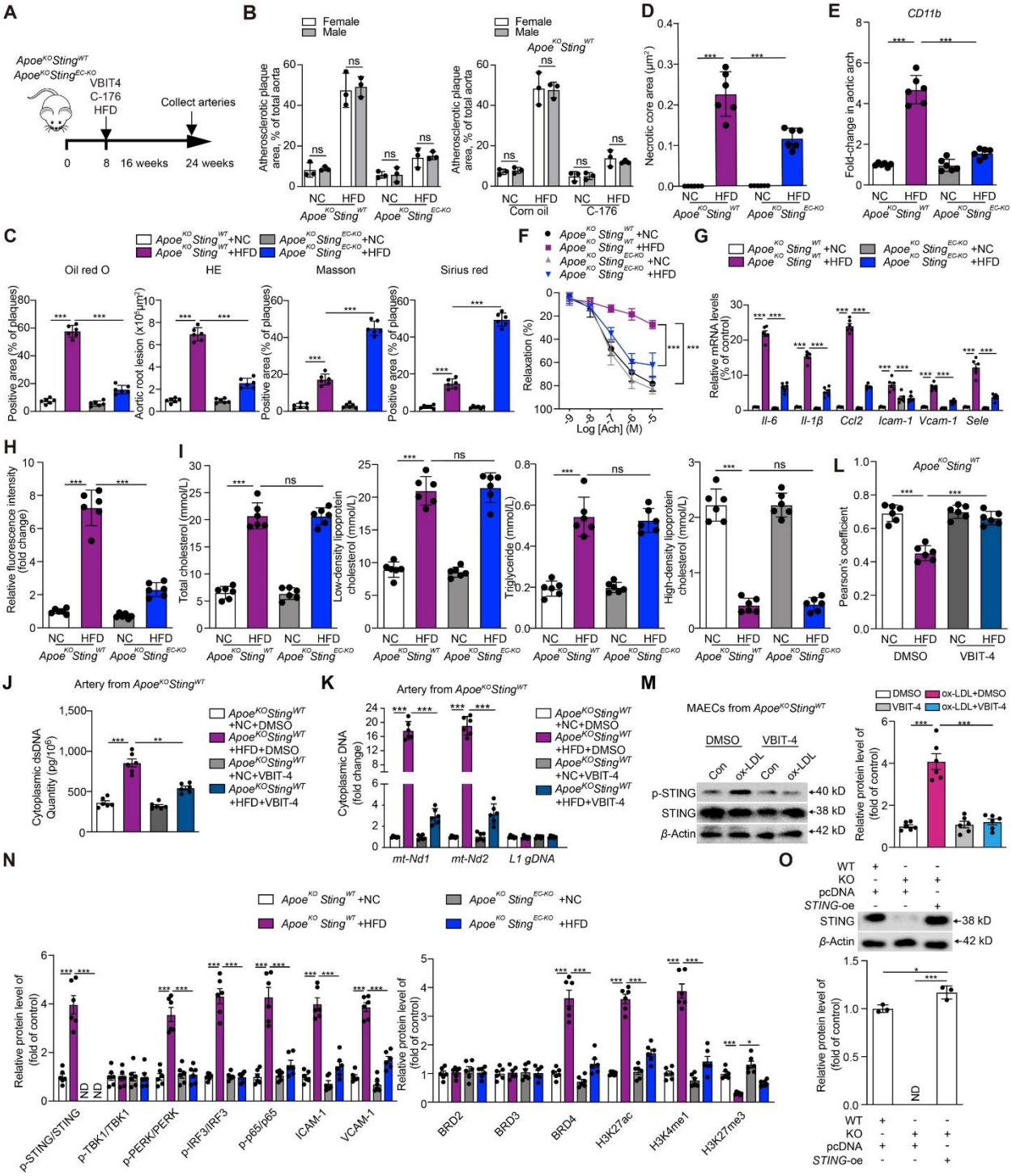

Figure S5 Endothelial deletion of STING could reverse the enhanced atherosclerotic lesions in *Apoe*^{KO}*Sting*^{WT} mice. (A) Study design. (B) The quantification of atherosclerotic plaque area of female and male *Apoe*^{KO} mice in each group treated as the Fig. 6A. (C) Quantification of oil red O, HE, Masson and Sirius red in Fig. 6B. (D) Quantification of necrotic core area of HE staining of aortic root of Fig. 6B. (E) The qRT-PCR analysis for the leukocyte marker CD11b on aortic arches of mice treated as Fig. 6B. (F)–(G) Ach-mediated endothelium-dependent relaxation (F), mRNA levels of inflammatory genes (G), in arteries from *Apoe*^{KO}*Sting*^{WT} and *Apoe*^{KO}*Sting*$^{EC\text{-}KO}$ mice fed with NC or HFD. (H) The quantification of ICAM-1 in

endothelium from *Apoe*^{KO}*Sting*^{WT} and *Apoe*^{KO}*Sting*$^{EC\text{-}KO}$ mice fed with NC or HFD in Fig. 6C. (I) The plasma content of total cholesterol, low density lipoprotein cholesterol, triglycerides and high density lipoprotein cholesterol from *Apoe*^{KO}*Sting*^{WT} and *Apoe*^{KO}*Sting*$^{EC\text{-}KO}$ mice fed with NC or HFD. (J)–(K) The cytoplasmic dsDNA concentration (J), the cytoplasmic expression of mtDNA, nuclear LINE1 elements and *RNA 18S* by qPCR (K) in the arteries from *Apoe*^{KO}*Sting*^{WT} mice fed with NC or HFD combined with VBIT-4. (L) Colocalization of mitochondria marker TOMM20 with dsDNA in Fig. 6H, measured using the Pearson's correlation coefficient. (M) The protein levels of total and phosphorylated STING in MAECs derived from *Apoe*^{KO}*Sting*^{WT} mouse thoracic aorta treated with ox-LDL and VBIT-4. (N) Quantification of western blot data of Fig. 6L. (O) Western blot analysis of overexpression efficiency targeting STING in MAECs from *Apoe*^{KO}*Sting*$^{EC\text{-}KO}$ mice. Data are shown as mean ± SEM, $n = 6$; *$P < 0.05$, **$P < 0.01$, ***$P < 0.001$; ND, not detected; ns, no significance.

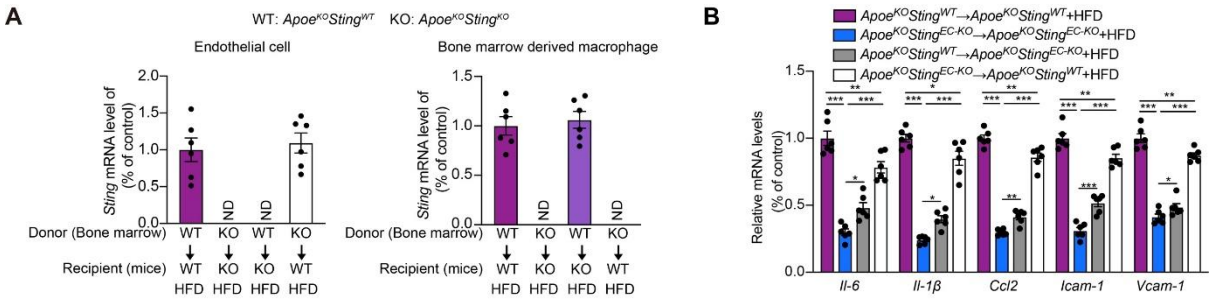

Figure S6 STING in endothelial cells plays a more important role than macrophages in promoting artery inflammation. (A) The *Sting* expression in endothelium and bone marrow derived macrophage of *Apoe*^{KO}*Sting*^{WT} and *Apoe*^{KO}*Sting*$^{EC\text{-}KO}$ mice involved in bone marrow transplantation by qRT-PCR. (B) Relative mRNA levels of inflammatory genes of aortas from *Apoe*^{KO} mice treated as in (Fig. 6O). Data are shown as mean ± SEM, $n = 6$; *$P < 0.05$, **$P < 0.01$, ***$P < 0.001$; ND, not detected.

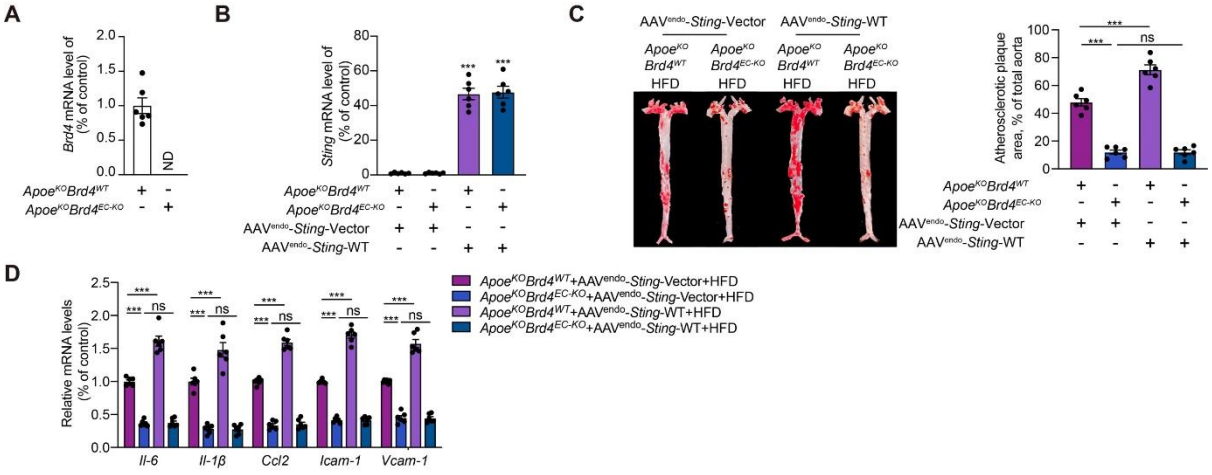

Figure S7 Endothelium overexpression of STING by AAV^{endo} could eliminate the deceased atherosclerotic lesions in *Apoe*^{KO}*Brd4*$^{EC\text{-}KO}$ mice. (A) Relative *Brd4* mRNA level in the endothelium of *Apoe*^{KO}*Brd4*^{WT} and *Apoe*^{KO}*Brd4*$^{EC\text{-}KO}$ mice. (B) Relative *Sting* mRNA level in the endothelium of *Apoe*^{KO}*Brd4*^{WT} and *Apoe*^{KO}*Brd4*$^{EC\text{-}KO}$ mice transfected with AAV^{endo}-*Sting*-Vector and AAV^{endo}-*Sting*-WT. (C) Representative images of en face aortas stained with oil red O from *Apoe*^{KO}*Brd4*^{WT} and *Apoe*^{KO}*Brd4*$^{EC\text{-}KO}$ mice fed with HFD transfected with AAV^{endo}-*Sting*-Vector and AAV^{endo}-*Sting*-WT. (D) The mRNA levels of inflammatory genes of aortas from *Apoe*^{KO} mice treated as in Supporting Information Fig. S7C. Data are shown as mean ± SEM, $n = 6$; ***$P < 0.001$; ND, not detected; ns, no significance.